Geographical variations of the $_0S_0$ normal mode amplitude: predictions and observations after the Sumatra-Andaman earthquake

Severine Rosat[1*], Shingo Watada[2], and Tadahiro Sato[1]

[1]National Astronomical Observatory of Japan, Mizusawa
[2]Earthquake Research Institute, University of Tokyo, Japan

(Received June 15, 2006; Revised October 23, 2006; Accepted December 1, 2006; Online published May 7, 2007)

The radial seismic normal mode $_0S_0$ was strongly excited by the 2004 Mw = 9.3 Sumatra-Andaman earthquake at a period of 20.5 min. In a spherically symmetric Earth model, $_0S_0$ amplitude is the same everywhere on the Earth's surface. However, when the ellipticity and rotation of the Earth are taken into consideration, theoretical computations predict an amplitude of $_0S_0$ 1% higher at the pole than at the equator. Based on a realistic three-dimensional heterogeneous rotating elliptic Earth model, our predictions indicate that the amplitude of $_0S_0$ is 2% higher at the pole than at the equator. A longitude dependency of $_0S_0$ amplitude is also shown. The analysis of 13 superconducting gravimeter (SG) records of the 2004 Sumatra-Andaman earthquake supports the predicted geographical variations of $_0S_0$ amplitude. We have also obtained new estimates for the frequency and Q of $_0S_0$: 0.8146566±1.6 10^{-6} mHz and 5506±19.

Key words: Seismic radial mode $_0S_0$, superconducting gravimeter, Sumatra-Andaman earthquake, lateral heterogeneities.

1. Introduction

After a strong excitation, such as an earthquake of a magnitude larger than 6.5, the Earth vibrates like a bell at different frequencies. These free oscillations are called the normal modes of the Earth, and they exhibit strong constraints on the Earth's density structure (Resovsky and Ritzwoller, 1998; Ishii and Tromp, 1999).

At the present time, 22 superconducting gravimeters (SGs) are continuously recording the time-varying surface gravity, and their measurements are collected in the framework of the Global Geodynamics Project (GGP) (Crossley *et al.*, 1999) since 1997. The high-resolution, low-noise level and stability of SGs at frequencies below 1 mHz (Van Camp, 1999; Widmer-Schnidrig, 2003; Rosat *et al.*, 2003, 2004) make these instruments suitable for the analysis of the low-frequency seismic normal modes of the Earth. The fundamental radial mode, $_0S_0$, called the "breathing mode" of the Earth, consists of an almost pure compression and dilatation of the Earth with a PREM (Dziewonski and Anderson, 1981) period of 20.5 min. The SG records are well calibrated so they present a good opportunity to study the normal modes amplitudes. In addition, the seismic mode $_0S_0$ has a unique eigenfrequency as it does not split, as in the case of an aspherical Earth. Therefore, its amplitude is free from the beating of splitting singlets. The geographical pattern of $_0S_0$ amplitude can therefore be used to examine the aspherical structures of the Earth. The strong excitation of $_0S_0$ after the 2004 M_w=9.3 Sumatra-Andaman earthquake provides a unique opportunity to further study this radial mode and to put new constraints on the Earth's models.

In this paper, we first present the $_0S_0$ surface amplitude predictions computed for a three-dimensional (3D) heterogeneous rotating elliptic Earth model. We then show that the measured $_0S_0$ amplitudes in 13 time-varying gravity SG records confirm the predicted geographical variations, and we also give new estimates of $_0S_0$ frequency and quality factor. The differences between observation and theory are discussed in the context of the results.

2. $_0S_0$ Surface Amplitude Predictions

In a spherically symmetric non-rotating Earth model such as PREM, the amplitude of $_0S_0$ is the same everywhere on the Earth's surface. However, when the rotation and ellipticity of the Earth is taken into account, the centrifugal force and the ellipticity cause the $_0S_0$ amplitude to have an apparent latitude dependency. While the elliptical Earth is oscillating at the period of $_0S_0$, the gravimeter moves up and down in the gravity field of the Earth. In this condition, the gravimeter records the free-air gravity change as well as the inertial acceleration. The free-air gravity change is 2*A*g/R (Dahlen and Tromp, 1998) where R is the radius of the Earth, g is the gravity and A is the motion amplitude of $_0S_0$. In the case of an elliptical rotating Earth model, the dependencies of g and R with latitude make the vertical gravity gradient smaller at the equator than at the pole. The variations in latitude of $_0S_0$ amplitude due to this effect alone are expected to be of 0.5% at the most.

For a complete estimation of $_0S_0$ surface amplitude variations, the coupling effect of $_0S_0$ with other seismic modes must also be considered. We have computed $_0S_0$ ampli-

*Now at The Royal Observatory of Belgium, Brussels, Belgium.

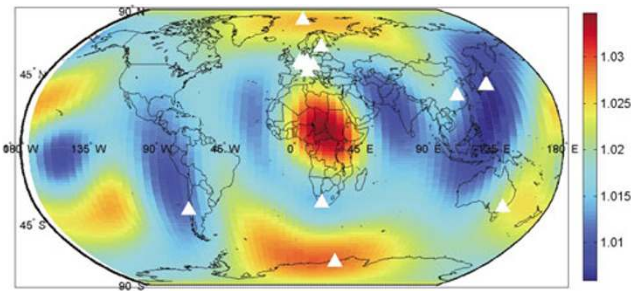

Fig. 1. Geographical distribution of the predicted $_0S_0$ amplitudes at the Earth's surface for a 3D SKS12WM13 rotating elliptic PREM model. The amplitude is normalized by $_0S_0$ amplitude for PREM. The white triangles represent the SG sites used in this study.

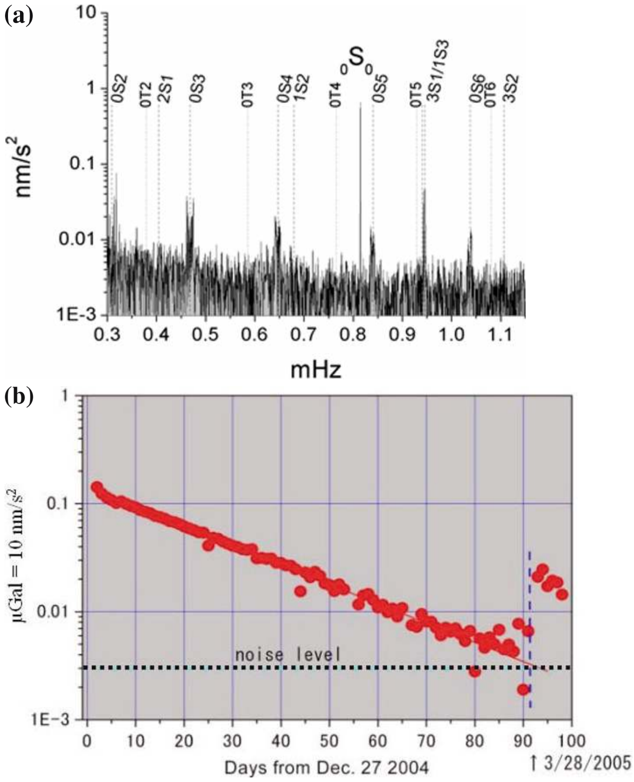

Fig. 2. (a) Amplitude spectrum on 34 days and (b) observed $_0S_0$ amplitude measured each day, after the 2004 Sumatra earthquake at Canberra SG site (revised from a figure by Y. Tamura).

tudes for a 3D rotating elliptic Earth based on a seismic shear wave velocity model SKS12WM13 (Dziewonski *et al.*, 1997) for the whole mantle, including the crustal boundaries undulations (Woodhouse and Dziewonski, 1984) and using a full coupling method. The SKS12WM13 velocity model is one of a group of models that describe a seismological mantle model required to compute the normal modes of the Earth; these include the crustal correction model, the shear-wave and compressional velocity models and the density model. An additional advantage of the SKS12WM13 velocity model is that it considers even and odd spherical harmonic order mantle structures. As we will show in following sections of this article, $_0S_0$ strongly couples with the $_0S_5$ mode through the spherical harmonic degree-five order structures. Therefore, the models limited to even order mantle structures are not adequate to compute the coupling of $_0S_0$. We have constructed the equation of motion of a rotating aspherical Earth following Woodhouse (1980) and sought its eigenfunctions and eigenfrequencies. In this method, both spherically symmetric and aspherical free oscillation problems are included into a large-scale generalized non-Hermitian eigenvalue problem (Watada *et al.*, 1993; Deuss and Woodhouse, 2001) without assuming a fiducial frequency. As a result, eigenfunctions and eigenfrequencies within a wide frequency range are obtained simultaneously. A feature of this method is that when the non-sphericity of the Earth approaches zero, the eigenfunctions and eigenfrequencies naturally come close to those of a spherically symmetric Earth model. In our computation, the Harvard CMT solution (http://www.seismology.harvard.edu/CMTsearch.html) has been adopted for the 2004 Sumatra-Andaman earthquake. Note that the absolute amplitude of $_0S_0$ is different for various source mechanisms but that its amplitude pattern remains the same.

All 22 spheroidal and toroidal multiplet modes below 1.32 mHz have been included in the mode-coupling computation. If we consider first the case of a spherically symmetric rotating elliptic Earth, $_0S_0$ strongly couples with the harmonic degree-two $_1S_2$, $_0S_2$ and $_2S_2$ modes - ordered by strength of coupling - through the elliptic figure of the Earth and with $_1T_1$ through the Coriolis force. The coupling effect through the rotation and ellipticity results in the amplitude of $_0S_0$ being higher at the pole than at the equator by 1% (compare Fig. 4, case of a laterally homogeneous rotating elliptic PREM model). When we introduce the lateral heterogeneities, modeled by the seismic shear wave SKS12WM13 model, $_0S_0$ strongly couples to $_0S_5$, which is the closest multiplet in the frequency domain. $_1S_2$, $_1S_3$, $_3S_2$ and $_0S_2$ also couple to $_0S_0$. In this case, we observe both a latitude and longitude dependency of $_0S_0$ amplitude at the Earth's surface. The geographical distribution of the computed $_0S_0$ amplitudes is given in Fig. 1. The difference between the minimum and maximum amplitudes reaches 2%. Note that the dominant degree-five pattern is due to the strong coupling of $_0S_0$ with $_0S_5$. Note also that the computation for the model SH12WM13 (Su *et al.*, 1994) gives a similar amplitude pattern of $_0S_0$.

3. Observed $_0S_0$ Amplitudes

The 2004 Sumatra-Andaman earthquake strongly excited $_0S_0$ (compare Fig. 2(a), example at Canberra SG site), and its amplitude decay could be observed up to the second Sumatra event in March 2005 (compare Fig. 2(b), example at Canberra SG site) at most SG sites that have a noise level of a few 10^{-2} nm/s^2 at $_0S_0$ frequency (Rosat *et al.*, 2005). The datasets from 13 GGP sites—Canberra (CB, Australia); Sutherland (SU, South Africa); Ny-Alesund (NY, Norway); Medicina (MC, Italy); Membach (MB, Belgium); Strasbourg (ST, France); Vienna (VI, Austria); Syowa (SY, Antarctica); Wettzell (WE), Bad-Homburg (BH) and Moxa (M1) (all in Germany); Kamioka (KA) and Matsushiro (MA) (both in Japan)—have been corrected for the local tides (solid tides and oceanic loading) and atmospheric

Table 1. Observed and predicted frequency and quality factor of ${}_0S_0$.

${}_0S_0$	frequency (mHz)	Q
Weighted mean of 13 SG records of 2004 Sumatra event	$0.8146566\pm1.6\ 10^{-6}$	5506 ± 19
Buland *et al.* (1979) (from 6 IDA records of 1977 Indonesian event)	$0.8146346\pm2.4\ 10^{-5}$	4100 ± 1066
Riedesel *et al.* (1980) (stacking of 9 IDA records)	$0.814664\pm3.3\ 10^{-6}$	5700 ± 285
Knopoff *et al.* (1979); Zürn *et al.* (1980) (from 2 ultra-long period seismographs)	$0.814674\pm9.0\ 10^{-6}$	6687 ± 869
Roult *et al.* (2006) (mean of 5 SG records of 2001 Peru event)	0.8146614	5489
PREM	0.8146639	5327

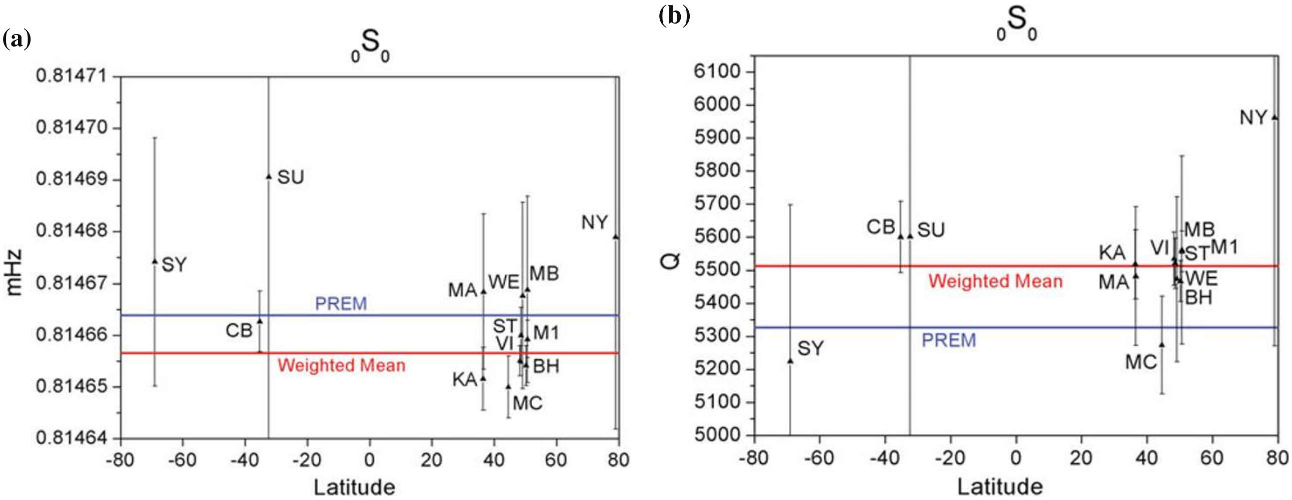

Fig. 3. Plot of the (a) frequency estimates and (b) Q estimates at each SG site. The weighted mean of the observations is plotted in the blue line and the PREM value in red.

pressure effect using a nominal admittance factor of -3 nm/s^2/hPa. The pressure correction is essential to reduce the noise level below 1 mHz (Zürn and Widmer, 1995; Van Camp, 1999; Rosat *et al.*, 2003; Widmer-Schnidrig, 2003). We have tested that the use of a nominal admittance instead of the actual barometric admittance does not affect the measured amplitude of ${}_0S_0$. For the Chilean station Tiga-Concepcion, continuous records were available up to January 1, following which gaps exist (in terms of several day gaps); we therefore did not use data from this site. Unfortunately, at that time, the equatorial station Bandung in Indonesia was out of order and, consequently, we have no SG record at the equator.

The estimation of ${}_0S_0$ frequency and Q using 34 days of 13 SG records is compared in Table 1 with PREM predictions and with previous observations. The 34-day record length is close to the 0.5-Q cycle for ${}_0S_0$ which is the optimal data length to measure the normal mode amplitude (Dahlen, 1982). The analysis method is similar to that used in Rosat *et al.* (2005). At each SG site, the frequency of ${}_0S_0$ has been estimated by fitting a Lorentzian function (Dahlen and Tromp, 1998) to the Hanning tapered FFT spectrum. The quality factor of ${}_0S_0$ has been estimated using a time-decay amplitude measurement (Roult and Clévédé, 2000). The errors have been evaluated based on the signal-to-noise ratio (SNR) following a method proposed by Dahlen (1982). The weighted means have then been computed. The new frequency and Q estimates of ${}_0S_0$ are more precise than those reported in previous studies (Table 1) because of the exceptionally large SNR of ${}_0S_0$ after the 2004 Sumatra event. ${}_0S_0$ frequency and Q at each SG site are plotted in Fig. 3.

The amplitude spectrum of ${}_0S_0$ has also been measured on 34-day records (from December 26 to January 28) at the 13 SG sites. Note that the spectral contamination from the Hanning tapered spectrum of the nearby ${}_0S_5$ mode can be safely ignored, as ${}_0S_5$ mode has a damping rate about 15-fold faster (Q=355 for PREM model) than ${}_0S_0$ and, consequently, it will quickly decay and not affect the spectral estimates using 34-day long data. The deviation from the mean value is represented as a function of the site latitude in Fig. 4 (black dots). The Esashi (Japan), Metsahovi (Finland) and Wuhan (China) sites are not plotted here, as the records are too noisy (error of 10% or more) due to some instrumental and environmental disturbances.

The error bars in Fig. 4 correspond to the error in the amplitude measurement of ${}_0S_0$ due to the presence of noise. The noise is the main source of error in ${}_0S_0$ amplitude measurement as SGs are well calibrated (see Discussion) and, therefore, the noise effect has been estimated from the SNR at each site. This error has been defined as $(s-s_0)/s_0$ where s is the measured amplitude of ${}_0S_0$, and s0 is the amplitude of ${}_0S_0$ after subtracting the noise. We also tested that the SNR of ${}_0S_0$ is not improved and that the ${}_0S_0$ amplitude deviations at the SG sites are the same for a data period longer than 34 days and for different time-windows.

Because we consider the deviations of ${}_0S_0$ amplitudes from the mean amplitude for both the observations as well as the predictions, the moment magnitude of the earthquake and the normalization of ${}_0S_0$ amplitudes used have no ef-

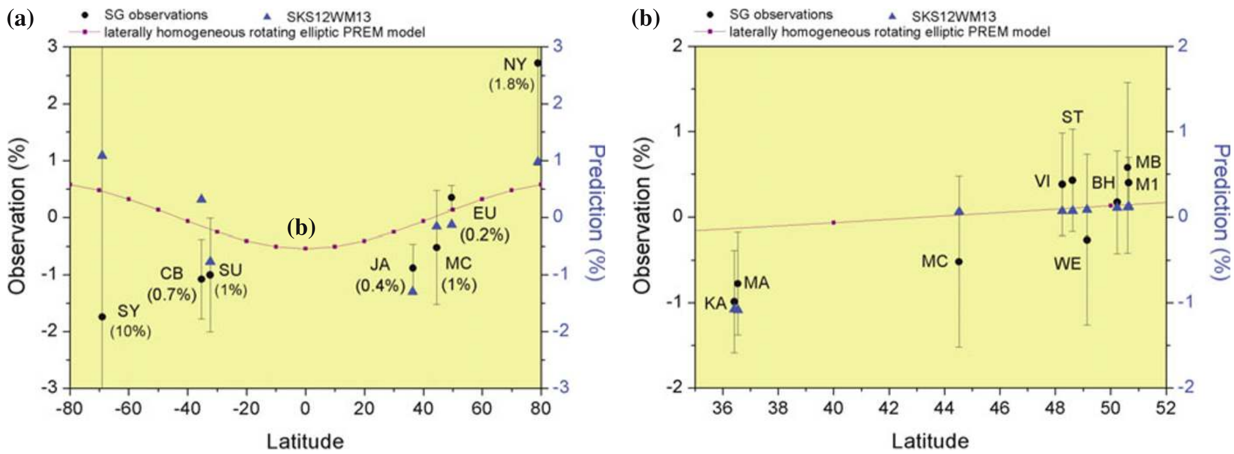

Fig. 4. Observed (black dots) and predicted (blue triangles) amplitude deviations of ${}_0S_0$ from the mean value at (a) 13 SG sites. The record length for the observations is 34 days. For the European sites (EU) VI, ST, WE, BH, MB and M1, and for the Japanese sites (JA) KA and MA, we have plotted the weighted mean; (b) zoom at mid-latitudes. The mean values for the observations and the predictions are different. ${}_0S_0$ amplitude deviation for a laterally homogeneous rotating elliptic Earth PREM model is also plotted as a function of latitude in purple. The error bars correspond to the effect of the noise with their values in parentheses.

fect on the results. For this same reason, although the predictions give the initial amplitude of ${}_0S_0$ at the time of the earthquake, because the measured ${}_0S_0$ spectral amplitude is obtained from the spectrum of 34-day SG records, there is no need to convert the observations to the initial excitation time. Notice that in terms of the predictions, the mean value has been computed from the predicted amplitudes at the SG sites in the same way as for the observations. The mean observed amplitude of ${}_0S_0$ is 0.66 nm/s^2.

4. Discussion

Calibration of the instrument is important in our comparison of the ${}_0S_0$ amplitude between the prediction and the observation. The SGs used in this study are well-calibrated using absolute gravimeters (e.g. Hinderer *et al.*, 1991; Tamura *et al.*, 2005) and lie at or below Peterson's low noise level (Peterson, 1993) at periods longer than 1000 s (Banka and Crossley, 1999; Rosat *et al.*, 2004). In addition, the anti-aliasing filters used for the acquisition at SG sites have a gain of one at ${}_0S_0$ frequency. Therefore, the calibration value can be safely applied at ${}_0S_0$ frequency. Indeed, the calibration error is 0.6% for NY (Sato *et al.*, 2006) and less than 0.3% for the other SGs (e.g. Amalvict *et al.*, 2001; Sato *et al.*, 2004). For the dual-sphere instruments at BH, WE and SU, the difference between the amplitudes measured from the lower and upper sphere records is also smaller than the noise effect. Using seismometers records, Davis (IRIS/IDA report, 2005) has observed about a 10% variation in the amplitude of ${}_0S_0$ in the global seismic data; although this is mainly due to calibration error, a portion is also due to noise, and the remainder should then be real effects due to lateral heterogeneities, including rotation and ellipticity.

As shown in Fig. 4, the predictions lie within the observation errors. SY is a very noisy site because of the tsunami effect (Nawa *et al.*, 2006). It is worth noting that KA and MA, located only 80 km apart, show very consistent amplitude deviations and are close to the predicted values. This same tendency can be noted for the European sites. Based on these results, we conclude that the observed values in the northern hemisphere support the predicted longitude dependency of ${}_0S_0$ amplitude due to the lateral heterogeneities inside the Earth. On the contrary, for the southern hemisphere site, CB, the observed ${}_0S_0$ amplitude deviation differs greatly from the predictions. Although the observation errors are still large, this difference may suggest that seismic tomographic models are less reliable in the southern Pacific region than in the northern hemisphere, possibly because of the sparse seismic station distribution. Another potential cause of the differences between SG observations and the predictions is that the tomographic model SKS12WM13 used here is a model for shear wave velocity Vs. To extract the compressional wave velocity V_p and the density perturbation ρ from V_s model, we have assumed two scale relationships between V_p, V_s and ρ: $d(\ln V_p)/d(\ln V_s)=0.8$ and $d(\ln \rho/d(\ln V_s)=0.4$. Ishii and Tromp (2001) have claimed that near the core-mantle boundary beneath central Pacific and Africa, there are two large regions of negative correlation between the density anomalies and S-wave anomalies, i.e. denser but with lower seismic velocity. There is a possibility that the difference between the observation and the prediction at CB site in Australia reflects the inaccurate scale relationship used in the tomographic model in this region.

A study of the sensitivity of the density structure on the surface amplitudes of ${}_0S_0$ is needed for further discussion. Such a sensitivity study requires computing the 3D amplitude kernels for the density (velocity) perturbations in the southern Pacific; hence, we have to study the kernel representation of the coupled normal modes. Such a study requires a theoretical development beyond the scope of our paper. In addition, the low number of SGs on the Earth's surface and the observation errors do not enable us to discuss in any detail the differences between observed and predicted ${}_0S_0$ amplitudes at the SG sites. However, we have reported the first evidence of the non-sphericity of ${}_0S_0$ observed directly from measurements and, based on the results, we can state that the precise measurement of normal mode amplitudes can provide some additional constraints on the seismic models.

5. Conclusion

We have presented the first observational evidence, supported by theoretical computation, of the geographical variation of $_0S_0$ amplitude, which is directly attributable to the accurate calibration and low noise level of SGs in the frequency range below 1 mHz. The development of more SG sites on the Earth's surface is necessary in order to be able to analyze further the latitude and longitude dependency of $_0S_0$ amplitude with the aim of constraining the lateral heterogeneities inside the Earth. A theoretical study of the horizontal component of the coupled $_0S_0$ oscillation should also highlight the non-sphericity pattern of $_0S_0$.

Acknowledgments. Part of this work was carried out with Grants in Aid for Scientific Research of the Ministry of Education, Culture, Sport, Science and Technology of Japan (MEXT): 16340134. S. Rosat is supported by the Japan Society for the Promotion of Science. The authors would like to thank the GGP managers for their records of the 2004 Sumatra-Andaman earthquake and the reviewers for their comments.

References

Amalvict, M., H. McQueen, and R. Govind, Absolute Gravity Measurements and Calibration of SG-CT031 at Canberra, 1999–2000, *J. Geodetic Soc. Jpn.*, **47**(1), 410–416, 2001.

Banka, D. and D. J. Crossley, Noise levels of superconducting gravimeters at seismic frequencies, *Geophys. J. Int.*, **139**, 87–97, 1999.

Buland, R., J. Berger, and F. Gilbert, Observations from the IDA network of attenuation and splitting during a recent earthquake, *Nature*, **277**, 358–362, 1979.

Crossley, D., J. Hinderer, G. Casula, O. Francis, H.-T. Hsu, Y. Imanishi, G. Jentzsch, J. Kaarianen, J. Merriam, B. Meurers, J. Neumeyer, B. Richter, K. Shibuya, T. Sato, and T. van Dam, Network of superconducting gravimeters benefits a number of disciplines, *EOS*, **80**, 121–126, 1999.

Dahlen, F. A., The effect of data windows on the estimation of free oscillations parameters, *Geophys. J. R. Astron. Soc.*, **69**, 537–549, 1982.

Dahlen, F. A. and J. Tromp, *Theoretical Global Seismology*, Princeton: Princeton University Press., Princeton, N.J., 1025 pp, 1998.

Davis, P., IRIS/IDA DCC report, DMS Standing Committee, web link: http://ida.ucsd.edu/pdf/GSNSC_2005_03.pdf 2005.

Deuss, A. and J. H. Woodhouse, Theoretical free-oscillation spectra: the importance of wide band coupling, *Geophys. J. Int.*, **146**, 833–842, 2001.

Dziewonski, A. M. and D. L. Anderson, Preliminary Reference Earth Model, *Phys. Earth Planet. Int.*, **25**, 297–356, 1981.

Dziewonski, A. M., X.-F. Liu, and W.-J. Su, Lateral heterogeneity in the lowermost mantle, in Earth's Deep Interior, edited by D. J. Crossley, (Cordon and Breach, Newark, N.J.), 11–49, 1997.

Hinderer, J., N. Florsch, J. Mäkinen, H. Legros, and J. E. Faller, On the calibration of the superconducting gravimeter using absolute gravity measurements, *Geophys. J. Int.*, **106**, 491–497, 1991.

Ishii, M. and J. Tromp, Normal-Mode and Free-Air Gravity Constraints on Lateral Variations in Velocity and Density of Earth's Mantle, *Science*, **285**, 1231-6, 1999.

Ishii, M. and J. Tromp, Even-degree lateral variations in the Earth's mantle constrained by free oscillations and the free-air gravity anomaly, *Geophys. J. Int.*, **145**, 77–96, 2001.

Knopoff, L., W. Zürn, P. A. Rydelek, and T. Yogi, Q of mode $_0S_0$, *J. of Geophys.*, **46**(2), 89–95, 1979.

Nawa, K., N. Suda, K. Satake, T. Sato, K. Doi, M. Kanao, and K. Shibuya, Loading and gravitational effects of the 2004 Indian Ocean tsunami observed at Syowa Station, Antarctica, BSSA, 2006 (submitted).

Peterson, J., Observations and modelling of seismic background noise, Open-File Report 93-332, U.S. Department of Interior, Geological Survey, Albuquerque, New Mexico, 1993.

Resovsky, J. S. and M. H. Ritzwoller, New and refined constraints on the three-dimensional Earth structure from normal modes below 3 mHz, *J. Geophys. Res.*, **103**(B1), 783–810, 1998.

Riedesel, M. A., D. Agnew, J. Berger, and F. Gibert, Stacking for the frequencies and Qs of $_0S_0$ and $_1S_0$, *Geophys. J. Roy. Astron. Soc.*, **62**, 457–471, 1980.

Rosat, S., J. Hinderer, and L. Rivera, First observation of $_2S_1$ and study of the splitting of the football mode $_0S_2$, *Geophys. Res. Lett.*, **30**, 21, 2111, 2003.

Rosat, S., J. Hinderer, D. Crossley, and J. P. Boy, Performance of superconducting gravimeters from long-period seismology to tides, *J. Geodyn.*, **38**(3-5), 461–476, 2004.

Rosat, S., T. Sato, Y. Imanishi, J. Hinderer, Y. Tamura, H. McQueen, and M. Ohashi, High resolution analysis of the gravest seismic normal modes after the 2004 Mw=9 Sumatra earthquake using superconducting gravimeter data, *Geophys. Res. Lett.*, **32**, L13304, doi:10.1029/2005GL023128, 2005.

Roult, G. and Clévédé, E, New refinements in attenuation measurements from free-oscillation and surface-wave observations, *Phys. Earth Planet. Int.*, **121**, 1–37, 2000.

Roult, G., S. Rosat, R. Millot-Langet, E. Clévédé, and J. Hinderer, New determinations of Q quality factors and eigenfrequencies for the whole set of singlets of the Earth's normal modes $_0S_0$, $_0S_2$, $_0S_3$ and $_2S_1$ using SG data from the GGP network, *J. Geodyn.*, **41**, 345–357, 2006.

Sato, T., Y. Tamura, K. Matsumoto, Y. Imanishi, and H. McQueen, Parameters of the fluid core resonance inferred from superconducting gravimeter data, *J. Geodyn.*, **38**, 375–389, 2004.

Sato, T., J.-P. Boy, Y. Tamura, K. Matsumoto, K. Asari, H.-P. Plag, and O. Francis, Gravity tide and seasonal gravity variations at Ny-Alesund, Svalbard in Arctic, *J. Geodyn.*, **41**, 234–241, 2006.

Su, W.- J., R. L. Woodward, and A. M. Dziewonski, Degree-12 model of shear velocity heterogeneity in the mantle, *J. Geophys. Res.*, **99**, 6945–6980, 1994.

Tamura, Y., T. Sato, Y. Fukuda, and T. Higashi, Scale factor calibration of a superconducting gravimeter at Esashi Station, Japan, using absolute gravity measurements, *J. Geodesy*, **78**, 481–488, 2005.

Van Camp, M., Measuring seismic normal modes with the GWR C021 superconducting gravimeter, *Phys. Earth Planet. Int.*, **116**, 81–92, 1999.

Watada, S., H. Kanamori, and D. L. Anderson, An analysis of Nearfield normal mode amplitude anomalies of the Landers earthquake, *Geophys. Res. Lett.*, **20**(23), 2611–2614, 1993.

Widmer-Schnidrig, R., What can superconducting gravimeters contribute to normal mode seismology?, *Bull. Seism. Soc. Am.*, **93**(3), 1370–1380, 2003.

Woodhouse, J. H., The coupling and attenuation of nearly resonant multiplets in the Earth's free oscillation spectrum, *Geophys. J. Roy. Astron. Soc.*, **61**, 261–283, 1980.

Woodhouse, J. H. and A. M. Dziewonski, Mapping the upper mantle: three dimensional modelling of Earth structure by inversion of seismic waveforms, *J. Geophys. Res.*, **89**, 5953–5986, 1984.

Zürn, W. and R. Widmer, On noise reduction in vertical seismic records below 2 mHz using local barometric pressure, *Geophys. Res. Lett.*, **22**, 3537–3540, 1995.

Zürn, W., L. Knopoff, and P. A. Rydelek, High precision measurement of the frequency of mode $_0S_0$, *J. Geophys.*, **48**(3), 158–160, 1980.

S. Rosat (e-mail: Severine.Rosat@oma.be), S. Watada, and T. Sato